Neuroinflammation induces nerve growth factor dependent nociceptor sensitisation in a neonatal rodent model of platinum-based chemotherapy induced neuropathic pain

Marlene Da Vitoria Lobo[b], Lydia Hardowar[a], Tameille Valentine [a], Lucy Tomblin[b], Charlotte Guest[a], Dhyana Sharma[a], Jasmine Elphick-Ross[a], Mark Paul-Clark[a], Richard Philip Hulse[a]*.

[a]Department of Biosciences, School of Science and Technology, Nottingham Trent University, Nottingham, NG11 8NS, [b]Division of Cancer and Stem Cells, School of Medicine, University of Nottingham, Nottingham NG7 2UH.

*Corresponding author
Corresponding Author Contact Details
Dr Richard P Hulse
Richard.Hulse@ntu.ac.uk
School of Science and Technology
New Hall Block
Nottingham Trent University
Clifton Lane
Nottingham
NG11 8NS

Richard.Hulse@ntu.ac.uk
https://orcid.org/0000-0002-5193-9822

Keywords: nociceptor, dorsal root ganglia, TrkA, chemotherapy, cisplatin, neurodegeneration, TRPV1

Data availability statement: All data is presented in this article and is available by reasonable request from the corresponding author.

Funding statement: This work was supported by the European Foundation for the Study of Diabetes Microvascular Programme supported by Novartis to RPH (Nov 2015_2 to RPH), the EFSD/Boehringer Ingelheim European Research Programme in Microvascular Complications of Diabetes (BI18_5 to RPH), the Rosetree Trust (A1360 to RPH) and Nottingham Trent University.

Author contribution statement: All researchers performed the experimental work and contributed to the conception or design of the work in addition to acquisition, analysis or interpretation of data for the work. All authors drafted the article or revised it critically for important intellectual content. All authors approved the final version of the manuscript.

Acknowledgements: The authors would like to thank Graham Hickman of the Imaging Suite at Nottingham Trent University for their support and assistance in this work.

Conflict of interest disclosure: Authors have nothing to disclose.

Ethics approval statement: This work has not been published or under review for publication elsewhere. All authors have seen and approved the final version of the abstract. All studies involving rodents were approved by local ethical review board at host institutions and in accordance with UK Home Office Legislation.

Abstract

Chemotherapy-induced peripheral sensory neuropathy (CIPN) is a highly prevalent adverse health related comorbidity that manifests later in life in adult patients who have undergone paediatric cancer treatment with chemotherapeutic agents. Symptoms are typified by induction of neuropathic pain in a larger proportion of these patients. There is limited understanding of how this cisplatin induced sensory neuropathy develops and as a consequence current treatment approaches are not effective. The mechanisms that cause cisplatin-induced survivorship pain have yet to be elucidated; however, recent studies have indicated the involvement a key component, TrkA receptor signalling. The aim of this study was to investigate the effect of cisplatin mediated neuroinflammation and the dependence upon cisplatin induced nociceptor sensitisation upon nerve growth factor signalling. In a rodent model of cisplatin induced survivorship pain, there was a prominent induction of neuroinflammatory process in the dorsal root ganglia, demonstrated by infiltration of NGF positive CD45 positive macrophages. Isolated mouse splenocytes exposed to cisplatin led to increases in NGF expression. Primary cell cultures of sensory neurons from the dorsal root ganglia of neonatal mice treated with cisplatin demonstrated enhanced TRPV1 mediated nociceptor activity, which was NGF dependent. In addition, conditioned media from cisplatin treated splenocytes similarly increased nociceptor activity, which was inhibited in a dose dependent manner following NGF monoclonal antibody incubation. Administration of monoclonal NGF antibody invivo prevented cisplatin induced survivorship pain in mice depicted by reductions in mechanical hypersensitivity as well as suppression of cisplatin induced aberrant nociceptor intraepidermal nerve fibre density. These results indicate that cisplatin treatment induces nociceptor activation via NGF mediated neuroinflammation. The present findings provide a basis on which future studies into NGF/TrkA signalling inhibition may prove to have clinical significance as a therapy for CIPN in adult survivors of childhood cancer.

Introduction

Cancer survivorship is increasingly prolonged due to medical advances in diagnosis and treatment. This is in particular demonstrated in patients whom were diagnosed with cancer during childhood, with 72% of children diagnosed with cancer living beyond 20years post diagnosis (REF). Unfortunately due to intensive and invasive nature of cancer treatment whether through surgical, radiotherapy, immunotherapy and chemotherapeutic approaches, patients suffer from extensive impact upon their quality of life. This is highlighted by adverse health related implications such as nephrotoxicity, optotoxicity, fatigue and negative emotive cognitive disorders as well as associated sociatal impact. In particular, adverse health related complication that arises as a consequence of treatment is chronic pain, which develops and persists into adulthood well beyond diagnosis and cessation of treatment. Persistant long lasting pain in childhood cancer survivors is prevalent in upto 59% of individuals and is attributed to the intensive nature of treatment [1,12]. Unfortunately as is common in most instances of chronic pain, current pain management is ineffective and therefore new treatment targets need to be identified in a disease dependent manner. There is an unmet clinical need in that the majority of ASCC experience pain. ASCC patients pain is a consequence of their cancer treatment[1]. There are no condition-tailored analgesics available for ASCC[2] as analgesia is predominantly ineffective and/or cause adverse side effects in the long-term. These difficulties arise due to analgesic management being based upon other neuropathic pain conditions[3] and a complete lack of understanding to what causes chronic pain in ASCC.

A front-line cancer treatment is platinum-based chemotherapy, which are effective against a range of solid tumours, including lung, bladder, testicular and ovarian cancers[7]. Cisplatin, in particular, has proven to be extremely effective in the treatment of metastatic testicular germ cell cancer, with a cure rate of over 90%. However, there are significant limitations to the use of these chemotherapy agents due to the severe, dose-limiting side effects of platinum-based chemotherapy treatments. A major dose-limiting, and potential cause for premature termination of treatment, is the neurotoxic effect of platinum-based chemotherapeutics on the peripheral nervous system. This cumulative sensory damage caused by chemotherapy treatment has been extensively reported to induce both immediate and delayed-onset pain sensations, that can manifest years after treatment cessation into adulthood [11,15,16]. It is recognised that in humans as well as in rodent models, chemotherapy damages and subsequently activates the sensory nerve fibres, driving chronic pain. It is important to note that the somatosensory nervous system is vulnerable at an early age to exposure to cellular stress/damage. If the somatosensory nervous system is exposed to an traumatic injury or inflammatory insult during neonatal development, pain hypersensitivity develops but is delayed with onset occurring during adolescence and persisting throughout adulthood [6]. This is thought to occur due to neuronal maladaptation to the neural stressor for example recently ourselves[9] and others[17] have developed suitable ASCC animal models that now allow us to investigate causative mechanisms and determine efficacy of analgesics. The development of this

delayed nociceptive behavioural phenotype is thought to arise from adaptations in the inflammatory system whereby proinflammatory events are typically impaired until later in life [14]. In these studies we demonstrate that cisplatin induced pain that occurs later life is NGF dependent due to a developing pro neuroinflammatory state within the dorsal root ganglia.

Methods

Ethical Approval and Animals used

All experimental procedures involving animals were carried out in consultation with local Animal Welfare and Ethics Review Board (University of Nottingham and Nottingham Trent University) and in accordance with UK Home office animals (Scientific procedures) Act 1986 and ARRIVE guidelines. Animals had ad libitum access to standard chow and were housed under 12:12h light:dark conditions.

Induction of Cisplatin induced neuropathic pain and administration of pharmacological agents

Neonatal Wistar rats were administered either vehicle (phosphate buffered saline; PBS) or cisplatin (Sigma-Aldrich; 0.1mg/kg) via intraperitoneal injection delivered on 2 occasions; postnatal (p) day 14 and 16. All rodents were weaned no later than 22 days and group housed according to gender. Males and female Wistar rats were utilised in all outlined studies. Body weight was monitored regularly throughout the study.

Nociceptive Behaviour

All rodents were habituated to the testing environments before nociceptive behavioural experimentation [4,23]. Mechanical withdrawal thresholds were scored following application of Von Frey (vF) hairs to the plantar surface of the hindpaw. This was calculated following application of differing vF filaments of increasing force a total of five times to the plantar surface of the hindpaw. Force response withdrawal curves were generated and mechanical withdrawal thresholds were determined as the mechanically applied force to elicit 50% of nociceptive withdrawals. The Hargreaves test was performed to determine heat nociceptive withdrawal latency [8]. A radiant heat source was applied to the plantar surface of the hindpaw. The duration (latency) between onset of stimulus to the mouse withdrawing their paws was recorded as the withdrawal latency. This was measured 3 times and a mean latency was calculated for both hindpaws.

Drug Delivery

1μM Nerve Growth Factor 2.5s (NGF, Alomone) was administered via a 20μl subcutaneous injection under recovery anaesthesia (~2% isoflurane in O_2). In some instances, NGF neutralising antibody was administered via intraperitoneal injection (0.1mg/kg) in phosphate buffered saline) versus IgG control.

Immunofluorescence

Animals from each experimental group were terminally anaesthetised (Dolethal; intraperitoneal sodium pentobarbital 200mg/ml). Animals were transcardially perfused with PBS and subsequently by 4% paraformaldehyde (PFA; pH7.4). Dorsal root ganglia (DRG) and hindpaw plantar sections

were extracted and cryopreserved in 30% sucrose. Tissues were stored at -80oC until processing [21]. Cryosections for DRG (8μm thickness) and plantar skin (20 μm thickness) sections were collected onto superfrost plus slides (VWR International). Slides were washed 3 times with PBS 0.4% Triton and then blocked with PBS, 0.2% Triton, 5% BSA (bovine serum albumin), and 10% FBS (foetal bovine serum) for 1 hour at room temperature. Sections were incubated at 4°C for 72 hours in blocking solution (5% bovine serum albumin, 0.2% Triton-X) containing primary antibodies CD45 antibody (Abcam, ab10558, 1:400 dilution), CD11b (Abcam), anti-NGF (Sigma Aldrich), IB4 (Sigma Aldrich was added in a 1:200 dilution). Sections were washed in PBS for 5 minutes three times. Secondary antibodies were subsequently applied to the tissue sections in PBS + 0.2% Triton X-100 at room temperature for 2 hours. CGRP immunoreactivity required an additional step to incorporate anti-rabbit biotinylated IgG (1 in 500, Jackson Laboratories 2hrs at room temperature) following by streptavidin alexafluor. Secondary antibodies (1:1000, all Invitrogen, UK) used were Alexa Fluor 555-conjugated donkey anti-mouse, Alexa Fluor 555-conjugated donkey anti-555, Alexa Fluor 555-conjugated donkey anti-rabbit, Alexa Fluor 488-conjugated donkey anti-rabbit and streptavidin-conjugated Alexa Fluor-555, (anti-rabbit 488, ab150073; anti-rabbit 555, ab15158; anti-mouse 555, ab150114; Streptavidin 555, S32355). Coverslips were mounted using vector laboratories H1000 meduim set mounting medium. Sections were imaged via confocal microscopy using a Leica confocal microscope.

Immunocytochemistry

Endothelial Cells; Coverslips from the 24 well plate were fixed with 1% PFA for 10 minutes. Then the wells were washed 3 times with PBS 0.1% BSA, followed by one wash of PBS 0.1% Tween, 3 more PBS/BSA washes and then blocked using the blocking solution. Primary antibodies for Occludin (Abcam, ab 31721), VE-cadherin (Abcam, ab33168), and ICAM-1 (Santa Cruz, XXX) were added for the different experiments in 1:100, 1:100, and 1:200 dilutions respectively and left overnight at 4 °C. Three washes with PBS/BSA were performed after the primary antibodies incubation. Secondary antibodies were added in a 1:500 dilution for 1 hour at room temperature. Three more washes were done and then the coverslips were carefully removed from the 24 well plate and placed in Super Frost slides (Sigma Aldrich) with a drop VectaShield. Coverslips were sealed with nail polish. All images were taken using the LAS X software from Leica Microsystems for confocal microscopy (TCS SPE confocal microscope).

Splenocyte adherence assay; Splenocytes from C57bl6 mice were labelled with Vybrant Dil before incubation with cisplatin-treated HUVEC. Splenocytes in suspension were incubated at 37 °C, 5% CO_2 with 5 μl of Vybrant Dil solution per ml of suspension for 20 minutes. Media was removed by centrifugation and the washing procedure was repeated twice. Splenocytes then were incubated with cisplatin treated HUVECs for 24 h at 37 °C, 5% CO_2 in a 24 well plate. The cells were then fixed with 1% PFA for 10 minutes and subsequently washed 5 times with PBS. Coverslips were

removed from the plate, placed in Super Frost slides with a drop of Vectashield and finally sealed with nail polish for confocal microscopy imaging. Splenocytes were extracted from C57bl6 mice and cultured in 50% endothelial media and 50% DMEM and RPMI respectively. Splenocytes were left in a T75 flask with fresh media and then transferred to a cell suspension before Vybant Dil (ThermoFisher) labelling.

Endothelial Cell Culture; Human umbilical vein endothelial cells (PromoCell C-12203) (HUVEC) were cultured and plated in either 6, 24 or 96 well plates. For Western blot analysis 50,000 cells per well were seeded on two 6 well plates. 2,000 cells per well were seeded in a 96 well plate for viability assays and 5,000 cells per well were seeded in a 24 well plate with ethanol sterilized coverslips for immunofluorescence assays. Cells were left to grow until they reach 90% confluency and then treated with cisplatin (0, 1, 3 or 5 µg/ml) for 24 hours.

Western Blot

Endothelial Cells; Protein from treated HUVEC was extracted using RIPA buffer (ThermoFisher) with 1X protease inhibitor cocktail (ThermoFisher, 78440) and sonication. Protein then was quantified using the Bradford assay and frozen until the western blot was performed. 10% Precast gels (Bio Rad) were loaded with 50 µg of protein per well. Gels were run at 90 V and stopped after 1 h 30 m. Semi wet transfer to a nitrocellulose membrane was made via Trans-Blot Turbo Transfer system (Bio Rad). Membranes were blocked with TBS 1% BSA, 0.1% Tween for 1 hour at 4 °C. Primary antibodies were used in a 1:200 dilution for ICAM-1 and β-actin and in a concentration of 1 µg/ml for VE-cadherin and occludin. Primary antibodies were left overnight at 4 °C. Three washes with TBS, 0.1% Tween were done after the incubation. Secondary antibodies were used in a 1:5000 dilution and were incubated for 1 h at room temperature. Five final washes with TBS, 0.1% Tween were performed and membranes were then analysed with the Licor Odissey.

Splenocytes; Protein lysate samples were extracted from mouse splenocytes. Splenocytes were plated into 6 well plates for at least 24h prior to cisplatin (5ug/ml) treatment. Cells were lysed using RIPA buffer (Sigma-Aldrich) containing protease inhibitor cocktail (Protease/Phosphastase inhibitor cocktail, Cell Signalling). Equal protein lysate concentrations (40µg per well) were loaded on a 4%-20% precast Mini-Protean gradient TGX gel (Biorad). Proteins were separated by SDS-PAGE electrophoresis and transferred to PVDF membranes using Trans-blot turbo transfer system (Bio-Rad). Membranes were incubated in 5% BSA in tris-buffered saline (TBS)-Tween 0.1% (TBST) for 1 hour at room temperature. Primary antibodies were incubated overnight at 4 ºC (NGF, CD45, B actin). The membrane was then incubated in secondary antibodies (Licor donkey anti-rabbit, anti goat and anti-mouse antibodies 1:10000) in TBST-0.1%- 1% BSA. Membranes were washes three times with TBST and visualised on the Licor Odyssey Fc.

Primary Dorsal Root Ganglia Sensory Neuronal Cell Culture

The reagents used in this study were as follows: Ham's F-12 Nutrient Nix with L-Glutamine, and N-2 Supplement (100X) (Gibco); Fluo-4, AM, cell permeant and Pluronic F-127 20% solution in dimethyl sulfoxide (DMSO) (Invitrogen); Dulbecco's phosphate-buffered saline (DPBS), bovine serum albumin (BSA) 30% in DPBS, laminin from Engelbreth-Holm-Swarm murine sarcoma basement membrane, 1-2 mg/mL in Tris-buffered saline, collagenase type XI 1.25%, and DMSO (Sigma-Aldrich); native mouse NGF 2.5S protein (>95%) (Alomone Labs); human b-NGF antibody (human, mouse, rat cross-reactivity) (R&D Systems); poly-L-lysine 0.01% in water (Merck Millipore). Cisplatin was used at a final concentration of 5µg/mL. Other reagents used include a 50mM stock of capsaicin made up in DMSO, penicillin-streptomycin (5000U/mL and 5000µg/mL), and HBSS containing calcium chloride, magnesium chloride, magnesium sulphate, potassium chloride, potassium phosphate, sodium bicarbonate, sodium chloride, sodium phosphate and glucose. C57BL/6 mice were housed and bred at Nottingham Trent University in accordance with the Animals (Scientific Procedures) Act 1986. A litter of mouse pups aged between postnatal day 7 to 14 were culled under Schedule 1 prior to dissection. Pups were chosen for this study, rather than adults, to better reflect the physiology and degree of nervous system development of human paediatric patients. A dorsal incision was made at the tail and continued in the cranial direction through the fur and skin to expose the spinal column. Adjacent ribs and connective tissues were removed to isolate the spinal column. The vertebrae were then removed, and the spinal cord extracted, to expose the DRGs within the column. The ganglia were then carefully extracted and the nerve roots trimmed off to minimise the presence of unwanted cell types in the subsequent culture. These ganglia were then placed in 1.8mL of Ham's F-12 media, supplemented with 0.5mL of 30% BSA, 1mL of penicillin/streptomycin (5000U/mL; 500µg/mL), and 0.5mL of 100X N-2 supplement.

One day prior to dissection, 75µL per well of poly-L-lysine was added to a 96-well plate and incubated overnight at 37°C; 5% CO2. The morning of dissection, the wells were washed with PBS, left to dry, then 100µL of 5µg/mL laminin in PBS was added to each well before incubating at 37°C; 5% CO2. 200µL of collagenase type IX was added to the 1.8mL of media containing the DRGs, in order to dissociate them from the cell ganglion and allow the individual neurons to be cultured in the wells. This was then incubated for 2 hours at 37°C; 5% CO2. This mixture was then triturated using a 1mL pipette tip to ensure the complete dissociation of the neurons, then 1mL of the cell suspension was added to each of two 15% BSA cushions (1mL Ham's F12 media + 1mL 30% BSA) in 15mL falcon tubes and centrifuged at 1200rpm for 8 minutes. This method filters out any cell debris remaining from dissection that could negatively affect the culture. The supernatants containing the cell debris, BSA and media was aspirated, and the cell pellets containing the neurons were resuspended in 1mL each and combined. 10µL of this suspension was added to one chamber of a C-Chip haemocytometer and the cell count calculated. Using this number the

necessary volume of media was added to the cell suspension in order to seed the cells at a concentration of 2000 cells per well. The seeded cells were kept incubated at 37°C; 5% CO2 and culture.

DRG Sensory Neuronal Calcium Assay

For the capsaicin dose-response experiments shown in Figure 2, doses of 0μM, 0.01μM, 0.1μM, 1μM, and 10μM capsaicin were used to validate the method and determine the appropriate concentration for stimulating a calcium response. 5x concentrations were made up in PBS, in order to achieve a 1x concentration when added to their neuron culture solution; 20μL of each dose of drug was added to the wells containing the neurons in 80μL of either PBS (Figures 1 and 2) or Hank's buffered saline solution (Figure 3) before immediately measuring the fluorescence response. The buffer used was changed as the PBS did not contain Ca2+ in solution to allow for an influx of Ca2+ into the neurons. For the NGF and antibody (Ab) series experiments shown in Figure 2, the treatments were set up as shown in Table 1. Final concentrations of NGF and capsaicin were 1nM and 1μM respectively. These treatments were done 24 hours prior to imaging. For the cisplatin treatments with NGF and antibody series shown in Figure 3, all treatment groups apart from vehicle (water) were treated with 5μg/mL cisplatin made up in supplemented F12 media one week prior to imaging. This was replaced with media only the following day. A day prior to imaging, NGF and Ab treatments were done as shown in Table 1.

24 hours after treatment with NGF and NGF antibody concentrations, the neurons were loaded with 100μL per well of Fluo-4 cell permeant in media containing 5μL DMSO and 5μL of 5% Pluronic, and incubated for 1 hour at 37°C; 5% CO2. Meanwhile, 5x capsaicin drug plates were made up as previously described, with 50μL of drug solution in wells corresponding to the correct treatment groups on the culture plate. The different reagents and concentrations used in each experiment are summarised in Table 2, where all capsaicin solutions were made up in PBS. The Fluo-4 was then replaced with 80μL of either PBS (Figures 1 and 2) or HBSS (Figure 3). Capsaicin was chosen to elicit a calcium response in these neurons as it is an agonist for the TRPV1 receptor, a nociceptor-specific receptor involved in pain perception. TRPV1 stimulation by capsaicin evokes a proportional increase in intracellular calcium, which was measured by the Infinite M Plex plate reader as a fluorescence response. 20μL of either drug or PBS (as control, see Figure 3) was added to the corresponding well of neurons and the fluorescence response per well measured at 10 second intervals over a 200 second time period. Prior to imaging, the plate reader was set to measure at 37°C to reflect physiological temperatures. The wavelength settings were selected based on the manufacturer specifications initially, then optimised using a confocal microscope to achieve the optimal wavelength settings of 488nm excitation and 516nm emission, with the gain set to 185. Baseline fluorescence readings were taken prior to each capsaicin treatment as t=0, with the subsequent timepoint readings expressed as a fold change over said baseline. This also

allowed for a more accurate representation of the change in fluorescence during the time delay of the plate reader that began producing readings after approximately 10 seconds.

Statistical Analysis

All data are represented as mean±SEM unless stated. Data were acquired and quantified using Microsoft Excel 2010, Image J (https://imagej.nih.gov/ij/) [18,19]and Graphpad Prism 8. Raw Ca2+ response values obtained using the plate reader were collated and background fluorescence removed by subtracting the smallest measured fluorescence value from each value in the dataset. These new values were then normalised by dividing by the fluorescence value obtained prior to capsaicin addition as a control, in order to determine the fold response over basal levels. For the capsaicin dose-response (Figure 2), a two-way ANOVA was employed to determine the treatment effect over time at different concentrations. For all other data sets, the effects of different treatments on the Ca2+ neuronal response were compared by either the area. Data was acquired and analysed using Microsoft Excel, Image J, Fiji, and GraphPad Prism 7. All images and gels were analysed using integrated density measurements and peak labelling from Image J or Fiji accordingly. T-student and one way ANOVA tests were used depending on the data retrieved from each experiment. P-values were calculated with GraphPad Prism 7. Graphs show mean and standard error bars. under the curve of each treatment group representing total response over the 200 second time period, or the maximum Ca2+ response measured at any time point. For these data sets, a oneway ANOVA with multiple comparisons was employed. All data are represented as mean ± SEM where $P<0.05$ is considered significant. Given n values represent the independent observations from each individual well containing the neuronal culture. Anomalous data points (over 2 standard deviations from the mean) were omitted. All statistical analysis was performed using GraphPad Prism version 8 for Mac.

Results

Early life administration of cisplatin induced a pronounced proinflammatory profile in the peripheral somatosensory nervous system; DRG and plantar skin at a timepoint accompanying presentation of pain (Fig.1). Cisplatin induced an increased infiltration and accumulation of CD45 (Fig.1 A&B) and CD11b (Fig1 C&D) positive immune cells into the plantar skin versus age matched vehicle controls (Fig. 1F&G). Additionally, cisplatin also induced CD45 (Fig. 1H-M) and GFAP ((Fig.1 I&J) positive immune cells accumulation in the lumbar dorsal root ganglia when compared to age matched vehicle controls. This infiltration and accumulation of CD45 and CD11b cell types in the peripheral somatosensory nervous system, was associated with alterations in endothelial cell function through cisplatin induced loss of tight junctional proteins (Fig.2A-C). This is alongside increased inflammatory cell-endothelial cell adherence that was associated with elevations in ICAM1 expression in cisplatin treated endothelial cells (HUVECs and spinal endothelial cells; Fig. 2E&F). In the plantar surface of the hindpaw of cisplatin treated rodents, there was an increase in CD45 inflammatory cell accumulation in association with microvessel endothelium (IB4 labelled) compared to age matched vehicle controls (Fig. 2G&H). Furthermore, infiltrating CD45 positive cell types in the dorsal root ganglia were positive for NGF in cisplatin treated rodents (Fig. 3 A-D) versus age matched controls. In isolated mouse splenocytes cisplatin induced increased expression of NGF versus vehicle treated groups (Fig. 3E-H).

NGF treatment led to increased capsaicin induced intracellular calcium influx (Fig. 4A) in DRG nociceptors. Furthermore, cotreatment with neutralising NGF-antibody inhibited NGF induced DRG nociceptor sensitisation, whereas IgG control did not suppress NGF induced nociceptor sensitisation (Fig. 4A). Subcutaneous administration in the hindpaw plantar surface of NGF with neutralising NGF antibody inhibited NGF induced mechanical (Fig.4B) and heat (Fig.4C) hypersensitivity in the ipsilateral hindpaw. Subcutaneous administration of NGF into the hindpaw plantar surface led to more abundant number of CGRP IENF in the ipsilateral plantar skin (representative image CGRP positive IENF Fig.4D) versus vehicle treated group. NGF administered inconjunction with NGF antibody, inhibited NGF induced increased number of CGRP positive IENF (Fig.4E).

DRG primary cell cultures were treated with cisplatin for 24hrs followed by a 7 day washout period. NGF induced TRPV1 sensitisation was exacerbated by cisplatin treatment, and treatment inconjunction with NGF neutralising antibody diminished NGF induced capsaicin responses compared to IgG control (Fig. 5A). Isolated mouse splenocytes were treated with either vehicle or cisplatin. Conditioned media was collected 24hrs later and applied to DRG primary cell cultures. Capsaicin induced intracellular calcium influx was increased in response to cisplatin treated conditioned media (Fig. 5B). Furthermore, with increasing concentrations of NGF neutralising

antibody cisplatin treated conditioned media induced nociceptor sensitisation was inhibited (Fig.5C). In a rodent model of early life cisplatin induced chronic pain that presents mechanical hypersensitivity, mechanical allodynia was prevented following intraperitoneal injection of NGF neutralising antibody (Fig. 6A). Furthermore, cisplatin induced increases in CGRP positive nociceptor IENF in the plantar skin was decreased in NGF neutralising antibody treated group (Fig. 6B-D). In addition, cisplatin induced accumulaton of CD45 positive cells in the plantar hindpaw skin was not altered by administration of NGF neutralising antibody (Fig. 6E&F).

Discussion

Current analgesics used to treat platinum-based sensory neuropathy provide little to no relief[2], with no systematic study designed to delineate suitable analgesia regimens for childhood cancer patients following anti-cancer treatment. Current analgesia efficacy has been based around alternative disease or treatment induced neuropathy with many drugs targeting central nervous system processing, whereas chemotherapy induced sensory neuropathy is deemed to be restricted[5] to the peripheral sensory nervous system (PNS). Key to the efficient function of the PNS is the supporting glial and inflammatory cell types, which secrete cytokines such as nerve growth factor (NGF). Activation of these cell types (neuroinflammation) is crucial to the development of chronic pain in adults as well as in children[9]. Inhibition of inflammatory signalling such as NGF and TNF alpha mediated pathways are currently targeted for analgesic development in arthritis. Cisplatin treatment drives inflammation in a multitude of systems, for instance in cisplatin induced nephropathy, whereby macrophage infiltration is associated with pathology progression. In addition, cisplatin has been shown to drive M1 macrophage polarisation and accompanying expression of pro-inflammatory agents TNF alpha and IL6. This is particularly pertinent as cisplatin induced survivorship pain is associated with an increased infiltration of CD45 cells and GFAP immunoreactivity restricted to the DRG; depicting neuroinflammatory activation. Suppression of this NGF-TrkA signalling prevents cisplatin induced activation of cisplatin induced nociceptor sensitisation and highlights that this signalling pathway is a putative target for treating survivorship pain.

The vast majority of work to date has focussed upon adult chemotherapy induced neuropathy, with childhood cancer survivorship pain underrepresented both in the clinic and at the basic research level. Analgesia is ineffective for children and adult patients. Our previous studies have demonstrated that alterations nociceptor activity following cisplatin treatment underlie the development of a platinum based delayed but lasting chronic pain. The immune system also plays a significant role in the mechanisms behind CIPN manifestation; cisplatin has been found to activate glial cells within the peripheral nervous system. This recruits immune cells to the area that release pro-inflammatory cytokines, such as chemokines (CKs) and interleukins (ILs). Studies have found that elevated levels of IL-1b, IL- 6, tumour necrosis factor-a (TNF-a) and nerve growth factor (NGF) as part of the inflammatory response associated with CIPN. The upregulation of these molecules is thought to stimulate the hyperexcitability and sensitisation of peripheral nociceptive neurons that cause the perceived pain sensation in CIPN patients. The dorsal root ganglia are particularly vulnerable to inflammatory damage due to a highly permeable protective barrier [10]. It also means that these neurons are particularly exposed to neurotoxic compounds, such as platinum-based chemotherapeutic agents. It has been identified that the DRG accumulated the highest concentrations of platinum of all the neural tissues when treated with cisplatin [13,20], and

that the resultant neurotoxic effects persisted long after cisplatin administration. Neurotoxicity and accompanying infiltration of differing inflammatory cell types promotes a proinflammatory environment within the dorsal root ganglia of cisplatin treated rodents. There have been extensive studies regarding peripheral sensitisation by varying inflammatory mediators in response to injury, including the role of NGF/TrkA signalling in the pathophysiology of peripheral sensory neuropathy. Many have determined the neurotoxic effects of platinum-based chemotherapy, and proposed various mechanisms by which these agents exert their allodynic and hyperalgesic effects. However, very few studies have specifically examined the effects of platinum-based drugs on NGF/TrkA-mediated nociceptor sensitisation. Further, although studies have demonstrated the development of chemotherapy-induced peripheral neuropathy in adult survivors of childhood cancer, there is very little literature regarding the mechanisms by which the treatment of paediatric patients leads to CIPN manifestation in adulthood. As NGF/TrkA signalling has been established as a key mediator in the development of neuropathic pain, inhibition of this pathway appears as an attractive target as a novel analgesic therapy. Preclinical studies have demonstrated the benefit of NGF/TrkA inhibition in relieving hyperalgesia and allodynia, which are the major symptoms suffered by CIPN patients[3]. Various approaches have been proposed regarding the mechanisms of action of such drugs, including inhibition of TrkA function, NGF/TrkA binding inhibition, and sequestration of free NGF. Although NGF/TrkA signalling has a widely acknowledged influence on peripheral sensitisation and associated pain development, very few studies have explored this pathway in the context of chemotherapy, particularly in relation to its effects on peripheral neurons of paediatric patients and how it leads to the manifestation of CIPN in adulthood. Hathway and colleagues investigated the effects of cisplatin treatment on the maturation of nociceptive systems in an in vivo rodent model and found an increase in TrkA+ neurons in the cisplatin-treated group [9]. Importantly, patients treated with cisplatin have been reported as having elevated serum NGF concentrations [22] highlighting that NGF-TrkA signalling axis as a prominent mediator of cisplatin induced neuropathic pain.

4.5. Conclusions

Our findings establish that NGF dependent modulation of cisplatin induced DRG nociceptor sensitisation and consequent development of chronic pain states. The results from this study indicate that cisplatin treatment exacerbates NGF mediated nociceptor sensitisation, and therefore acts as a key mediator in increased pain perception in chemotherapy-induced pain in adult survivors of childhood cancer. Furthermore, the present findings demonstrate the clinical relevance of developing an antibody-based novel analgesic to inhibit NGF mediated nociceptor signalling, in order to treat the painful symptoms of chemotherapy induced peripheral neuropathy in childhood survivors of cancer.

Figure Legends

Figure 1. Cisplatin induced DRG macrophage infiltration. Following early life exposure of cisplatin led to an increase in a proinflammatory environment in the plantar skin of the hindpaw. There was [A&B] an increase in CD45 positive cells types in the plantar skin of the hindpaw in cisplatin treated rodents versus age matched sham control [F]. Similarly, [C&D] there was an increase in CD11b positive cells in the plantar skin of the hindpaw in cisplatin rodents versus age matched sham control rodents[G]. Representative images of [H] no primary control and [I] naïve versus [J] cisplatin DRG demonstrated CD45 immunoreactivity. [K] In the dorsal root ganglia (lumbar 5) there was an increase in CD45 positive cells in cisplatin rodents when compared to age matched sham controls. (*P<0.05 Unpaired T Test). Representative images of [L] naïve versus [J] cisplatin DRG demonstrated GFAP immunoreactivity. [M] In the dorsal root ganglia (lumbar 5) there was an increase in GFAP positive cells in cisplatin rodents when compared to age matched sham controls. (*P<0.05 Unpaired T Test).

Figure 2 – Cisplatin induced dorsal root ganglia inflammatory environment
[A] HUVECs were treated with vehicle or cisplatin leading to reductions in endothelial tight junctional markers (VE Cadherin and Occludin). Protein extracted from HUVEC after 24h treatment with 0, 1, 3 or 5 g/ml of cisplatin demonstrated reductions in [B] VE Cadherin and [C] Occludin expression. Immunocytochemistry of HUVECs treated for 24hrs with either vehicle or cisplatin demonstrated reductions in [D] VE-Cadherin and [E] increases in ICAM1. [F] Cisplatin-induced [G] increases in ICAM-1 expression in HUVECs and mouse spinal cord endothelial cells. [H] In rodents treated with cisplatin had increased accumulation CD45 cells in the plantar skin that were associated with IB4 microvessels versus age matched control animals.

Figure 3 – Cisplatin induced accumulation of NGF positive monocyte/macrophages in the dorsal root ganglia
In rodents treated with cisplatin early in life presented increased numbers of NGF positive cells in the dorsal root ganglia ([A&B] representative images versus age matched vehicle control animals [C&D]. Isolated mouse splenocytes treated with either vehicle or cisplatin for 24hrs led to [E representative western blot &F] increased expression of NGF following cisplatin treatment and increased number of cells expressing NGF [G&H].

Figure 4 - Neutralising antibody suppression in NGF induced nociceptor senstisation and aberrant growth
Isolated DRG primary neuronal cell cultures [A] NGF induced increase capsaicin mediated intracellular calcium influx. This was suppressed with increasing concentrations of NGF

neutralising antibody. Data shown as mean ± SEM, n=16 for PBS and NGF + 0μg/mL Ab treatment groups, n=14 for vehicle treatment, n=10 for NGF + 0.1μg/mL, 0.3μg/mL, 1μg/mL and 2μg/mL antibody treatment groups. [B] Subcutaneous injection of NGF plus neutralising antibody preventing NGF induced [B] mechanical and [C] heat hyperalgesia, [D&E] alongside reductions in NGF induced CGRP nociceptor IENF aberrant growth versus NGF treatment.

Figure 5 – Cisplatin induced proinflammatory mediated nociceptor sensitisation is NGF dependent [A] Treatment of with 5μg/mL cisplatin 1 week prior to NGF treatment increased total (AUC) compared to vehicle. NGF neutralising antibody diminished capsaicin induced TRPV1 mediated nociceptor activity. [B] Conditioned media from cisplatin treated mouse splenocytes led to increased capsaicin evoked DRG nociceptor activity compared vehicle treated conditioned media, [C] which was diminished with increasing concentrations NGF neutralising antibody.

Figure 6 – NGF mediated cisplatin induced survivorship pain
In a rodent model of early life exposure of cisplatin induced chronic pain [A] intraperitoneal injection of neutralising antibody prevented mechanical allodynia versus cisplatin + vehicle group. Furthermore, [B representative pictures] CGRP nociceptor IENF was [C&D] increased by cisplatin, which was prevented by NGF neutralising antibody. Proinflammatory state [E representative images of CD45 positive cell infiltration] within the plantar skin remained [F] unchanged across vehicle, cisplatin and cisplatin + NGF antibody

References

[1] Alberts NM, Gagnon MM, Stinson JN. Chronic pain in survivors of childhood cancer: a developmental model of pain across the cancer trajectory. Pain 2018. doi:10.1097/j.pain.0000000000001261.

[2] Argyriou AA, Koutras A, Polychronopoulos P, Papapetropoulos S, Iconomou G, Katsoulas G, Makatsoris T, Kalofonos HP, Chroni E. The impact of paclitaxel or cisplatin-based chemotherapy on sympathetic skin response: A prospective study. Eur J Neurol 2005;12:858–861.

[3] Bloom AP, Jimenez-Andrade JM, Taylor RN, Castaneda-Corral G, Kaczmarska MJ, Freeman KT, Coughlin KA, Ghilardi JR, Kuskowski MA, Mantyh PW. Breast cancer-induced bone remodeling, skeletal pain, and sprouting of sensory nerve fibers. J Pain 2011;12:698–711. doi:10.1016/j.jpain.2010.12.016.

[4] Drake RA, Steel KA, Apps R, Lumb BM, Pickering AE. Loss of cortical control over the descending pain modulatory system determines the development of the neuropathic pain state in rats. Elife 2021;10.

[5] Ferdousi M, Azmi S, Petropoulos IN, Fadavi H, Ponirakis G, Marshall A, Tavakoli M, Malik I, Mansoor W, Malik RA. Corneal confocal microscopy detects small fibre neuropathy in patients with upper gastrointestinal cancer and nerve regeneration in chemotherapy induced peripheral neuropathy. PLoS One 2015;10.

[6] Fitzgerald M. The development of nociceptive circuits. Nat Rev Neurosci 2005;6:507–520. doi:10.1038/nrn1701.

[7] Gilchrist LS, Tanner L. The pediatric-modified total neuropathy score: a reliable and valid measure of chemotherapy-induced peripheral neuropathy in children with non-CNS cancers. Support Care Cancer 2013;21:847–856. doi:10.1007/s00520-012-1591-8.

[8] Hargreaves K, Dubner R, Brown F, Flores C, Joris J. A new and sensitive method for measuring thermal nociception in cutaneous hyperalgesia. Pain 1988;32:77–88.

[9] Hathway GJ, Murphy E, Lloyd J, Greenspon C, Hulse RP. Cancer Chemotherapy in Early Life Significantly Alters the Maturation of Pain Processing. Neuroscience 2017.

[10] Jimenez-Andrade JM, Herrera MB, Ghilardi JR, Vardanyan M, Melemedjian OK, Mantyh PW. Vascularization of the dorsal root ganglia and peripheral nerve of the mouse: Implications for chemical-induced peripheral sensory neuropathies. Mol Pain 2008;4:1–8.

[11] Khan RB, Hudson MM, Ledet DS, Morris EB, Pui CH, Howard SC, Krull KR, Hinds PS, Crom D, Browne E, Zhu L, Rai S, Srivastava D, Ness KK. Neurologic morbidity and quality of life in survivors of childhood acute lymphoblastic leukemia: a prospective cross-sectional study. J Cancer Surviv 2014;8:688–696.

[12] Lu Q, Krull KR, Leisenring W, Owen JE, Kawashima T, Tsao JC, Zebrack B, Mertens A, Armstrong GT, Stovall M, Robison LL, Zeltzer LK. Pain in long-term adult survivors of childhood cancers and their siblings: a report from the Childhood Cancer Survivor Study. Pain 2011;152:2616–2624. doi:10.1016/j.pain.2011.08.006.

[13] McDonald ES, Randon KR, Knight A, Windebank AJ. Cisplatin preferentially binds to DNA in dorsal root ganglion neurons in vitro and in vivo: a potential mechanism for neurotoxicity. Neurobiol Dis 2005;18:305–313. doi:10.1016/j.nbd.2004.09.013.

[14] McKelvey R, Berta T, Old E, Ji RR, Fitzgerald M. Neuropathic pain is constitutively suppressed in early life by anti-inflammatory neuroimmune regulation. J Neurosci 2015;35:457–466.

[15] Ness KK, Jones KE, Smith WA, Spunt SL, Wilson CL, Armstrong GT, Srivastava DK, Robison LL, Hudson MM, Gurney JG. Chemotherapy-related neuropathic symptoms and functional impairment in adult survivors of extracranial solid tumors of childhood: results from the St. Jude Lifetime Cohort Study. Arch Phys Med Rehabil 2013;94:1451–1457.

[16] Phillips SM, Padgett LS, Leisenring WM, Stratton KK, Bishop K, Krull KR, Alfano CM, Gibson TM, de Moor JS, Hartigan DB, Armstrong GT, Robison LL, Rowland JH, Oeffinger KC, Mariotto AB. Survivors of Childhood Cancer in the United States: Prevalence and Burden of Morbidity. Cancer Epidemiology Biomarkers & Prevention 2015;24:653–663. doi:10.1158/1055-9965.epi-14-1418.

[17] Schappacher KA, Styczynski L, Baccei ML. Early life vincristine exposure evokes mechanical pain hypersensitivity in the developing rat. Pain 2017;158:1647–1655. doi:10.1097/j.pain.0000000000000953.

[18] Schindelin J, Arganda-Carreras I, Frise E, Kaynig V, Longair M, Pietzsch T, Preibisch S, Rueden C, Saalfeld S, Schmid B, Tinevez JY, White DJ, Hartenstein V, Eliceiri K, Tomancak P, Cardona A. Fiji: An open-source platform for biological-image analysis. Nat Methods 2012;9:676–682. doi:10.1038/nmeth.2019.
[19] Schneider CA, Rasband WS, Eliceiri KW. NIH Image to ImageJ: 25 years of image analysis. Nat Methods 2012;9:671–675.
[20] Ta LE, Espeset L, Podratz J, Windebank AJ. Neurotoxicity of oxaliplatin and cisplatin for dorsal root ganglion neurons correlates with platinum-DNA binding. Neurotoxicology 2006;27:992–1002. doi:10.1016/j.neuro.2006.04.010.
[21] Ved N, Lobo MEDV, Bestall SM, Vidueira CL, Beazley-Long N, Ballmer-Hofer K, Hirashima M, Bates DO, Donaldson LF, Hulse RP. Diabetes-induced microvascular complications at the level of the spinal cord; a contributing factor in diabetic neuropathic pain. J Physiol 2018;596:3675–3693. doi:10.1113/JP275067.
[22] Velasco R, Navarro X, Gil-Gil M, Herrando-Grabulosa M, Calls A, Bruna J. Neuropathic Pain and Nerve Growth Factor in Chemotherapy-Induced Peripheral Neuropathy: Prospective Clinical-Pathological Study. J Pain Symptom Manage 2017;54:815–825.
[23] da Vitoria Lobo ME, Weir N, Hardowar L, al Ojaimi Y, Madden R, Gibson A, Bestall SM, Hirashima M, Schaffer CB, Donaldson LF, Bates DO, Hulse RP. Hypoxia induced carbonic anhydrase mediated dorsal horn neuron activation and induction of neuropathic pain. Pain 2022;163:2264–2279.

Figure 1

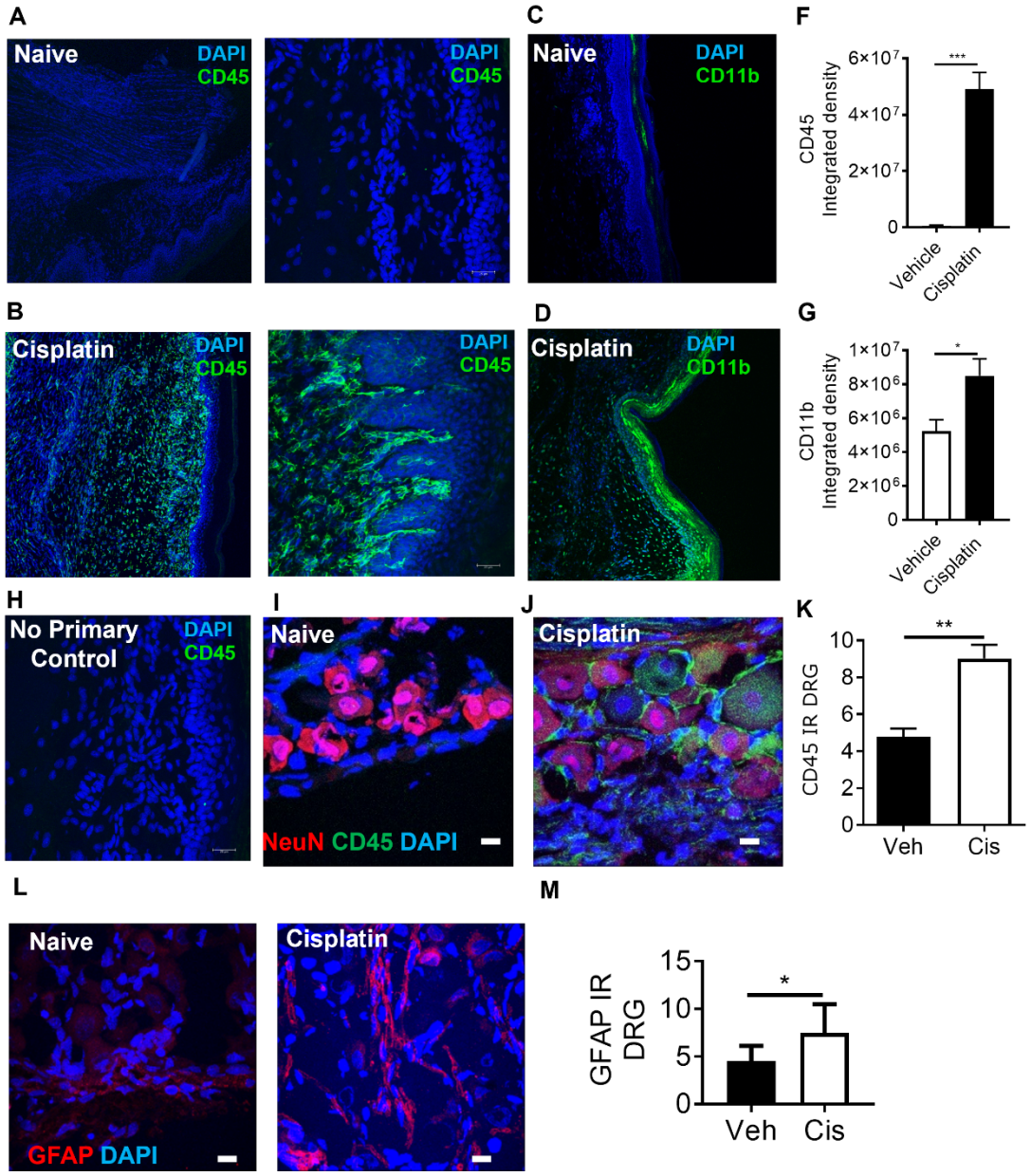
A
Naive
DAPI
CD45
DAPI
CD45
C
Naive
DAPI
CD11b
F
CD45
Integrated density
6×10^7
4×10^7
2×10^7
0
***
Vehicle
Cisplatin
B
Cisplatin
DAPI
CD45
DAPI
CD45
D
Cisplatin
DAPI
CD11b
G
CD11b
Integrated density
1×10^7
8×10^6
6×10^6
4×10^6
2×10^6
0
*
Vehicle
Cisplatin
H
No Primary
Control
DAPI
CD45
I
Naive
NeuN CD45 DAPI
J
Cisplatin
K
CD45 IR DRG
10
8
6
4
2
0
**
Veh
Cis
L
Naive
GFAP DAPI
Cisplatin
M
GFAP IR
DRG
15
10
5
0
*
Veh
Cis

Figure 2

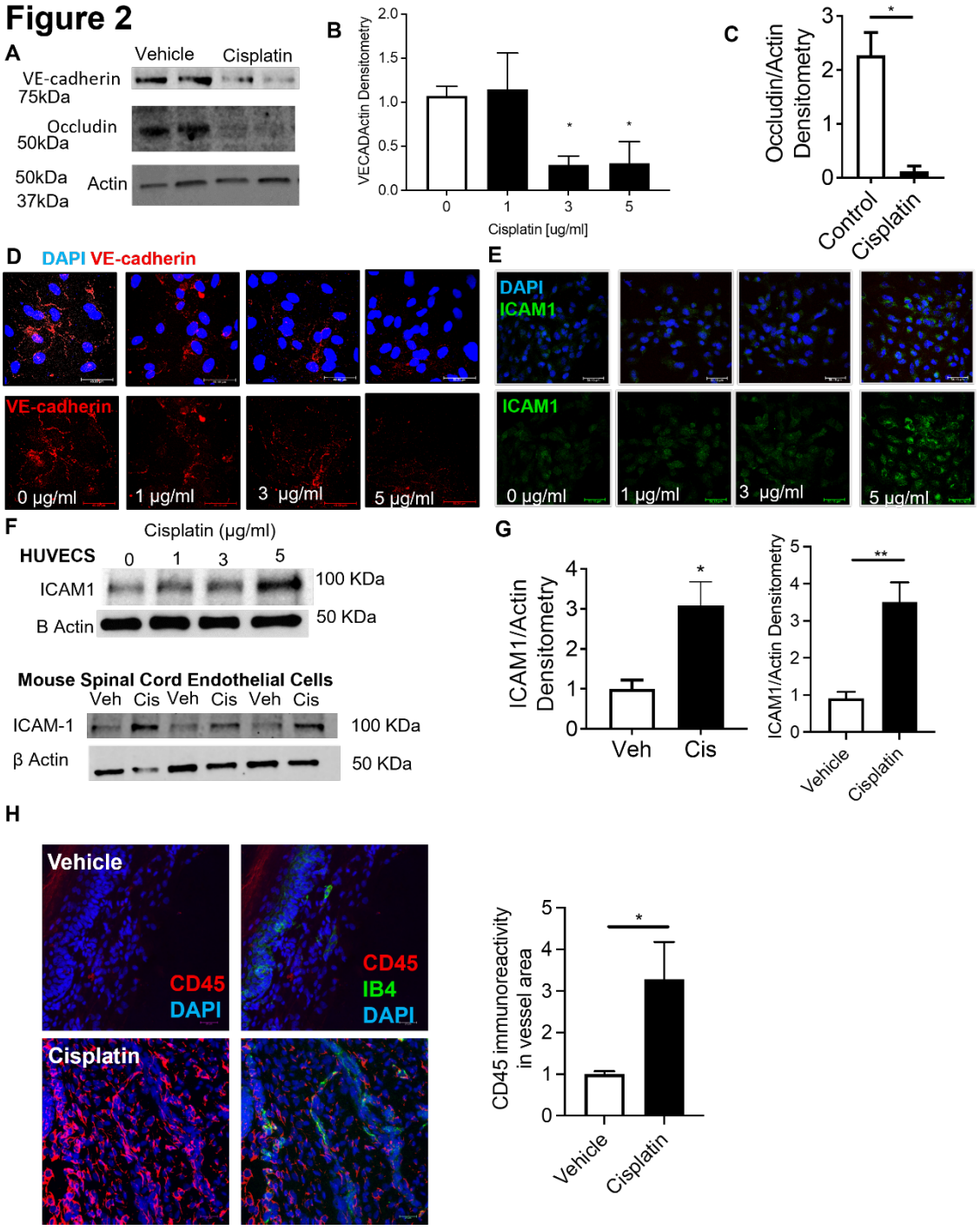
A
Vehicle
Cisplatin
VE-cadherin
75kDa
Occludin
50kDa
50kDa
37kDa
Actin
B
VECADActin Densitometry
2.0
1.5
1.0
0.5
0.0
0
1
3
5
Cisplatin [ug/ml]
C
Occludin/Actin Densitometry
3
2
1
0
Control
Cisplatin
D
DAPI VE-cadherin
VE-cadherin
0 µg/ml
1 µg/ml
3 µg/ml
5 µg/ml
E
DAPI
ICAM1
ICAM1
0 µg/ml
1 µg/ml
3 µg/ml
5 µg/ml
F
Cisplatin (µg/ml)
HUVECS
0
1
3
5
ICAM1
100 KDa
B Actin
50 KDa
Mouse Spinal Cord Endothelial Cells
Veh Cis Veh Cis Veh Cis
ICAM-1
100 KDa
β Actin
50 KDa
G
ICAM1/Actin Densitometry
4
3
2
1
0
Veh
Cis
ICAM1/Actin Densitometry
5
4
3
2
1
0
Vehicle
Cisplatin
H
Vehicle
CD45
DAPI
CD45
IB4
DAPI
Cisplatin
CD45 immunoreactivity in vessel area
5
4
3
2
1
0
Vehicle
Cisplatin

Figure 3

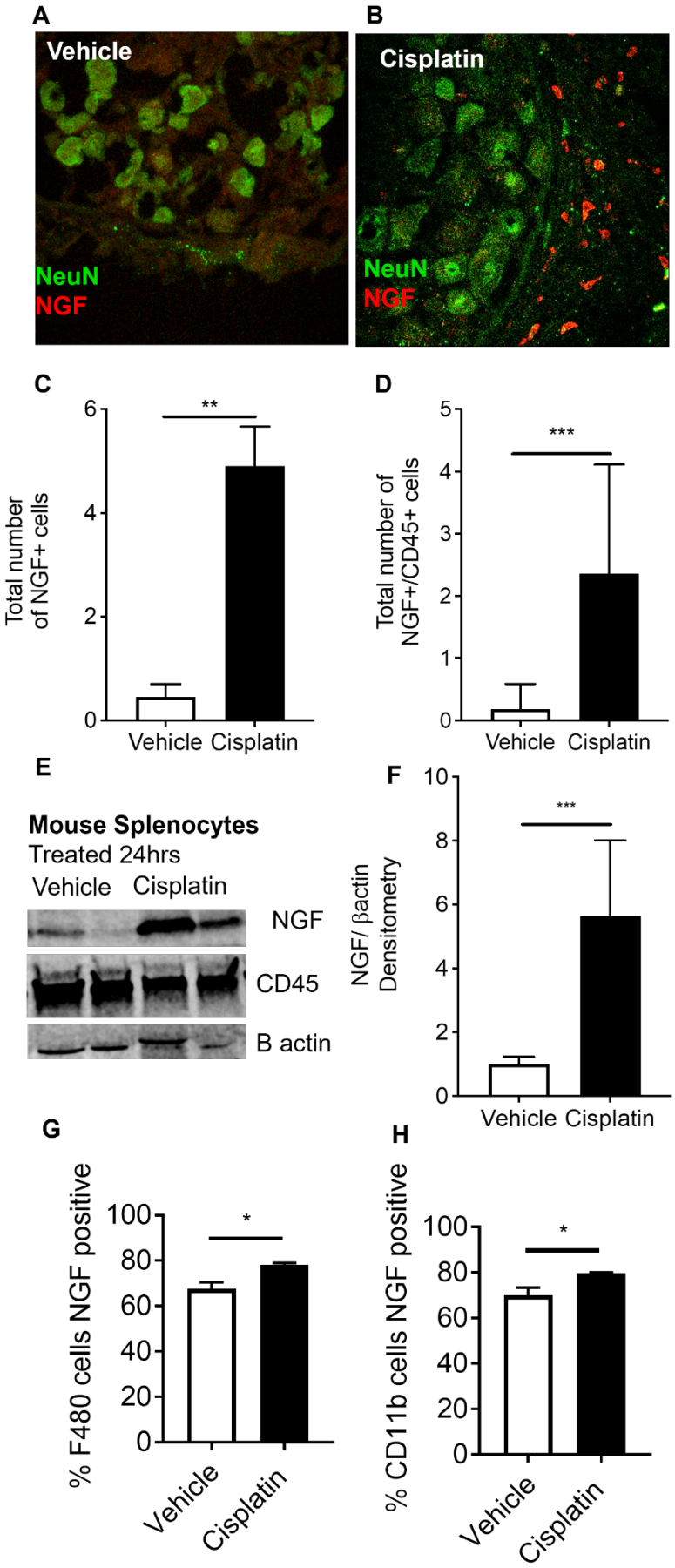
A
Vehicle
NeuN
NGF
B
Cisplatin
NeuN
NGF
C
Total number of NGF+ cells
**
Vehicle
Cisplatin
D
Total number of NGF+/CD45+ cells
***
Vehicle
Cisplatin
E
Mouse Splenocytes
Treated 24hrs
Vehicle
Cisplatin
NGF
CD45
B actin
F
NGF/ βactin Densitometry
***
Vehicle
Cisplatin
G
% F480 cells NGF positive
*
Vehicle
Cisplatin
H
% CD11b cells NGF positive
*
Vehicle
Cisplatin

Figure 4

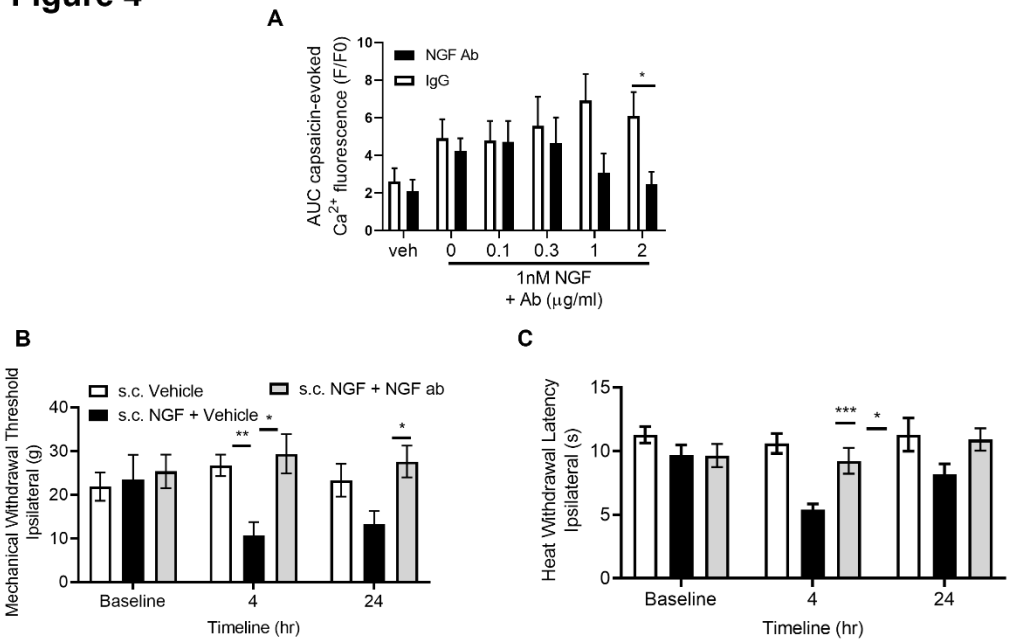
A
AUC capsaicin-evoked
Ca2+ fluorescence (F/F0)
NGF Ab
IgG
veh
0
0.1
0.3
1
2
1nM NGF
+ Ab (μg/ml)
B
Mechanical Withdrawal Threshold
Ipsilateral (g)
s.c. Vehicle
s.c. NGF + Vehicle
s.c. NGF + NGF ab
Baseline
4
24
Timeline (hr)
C
Heat Withdrawal Latency
Ipsilateral (s)
Baseline
4
24
Timeline (hr)

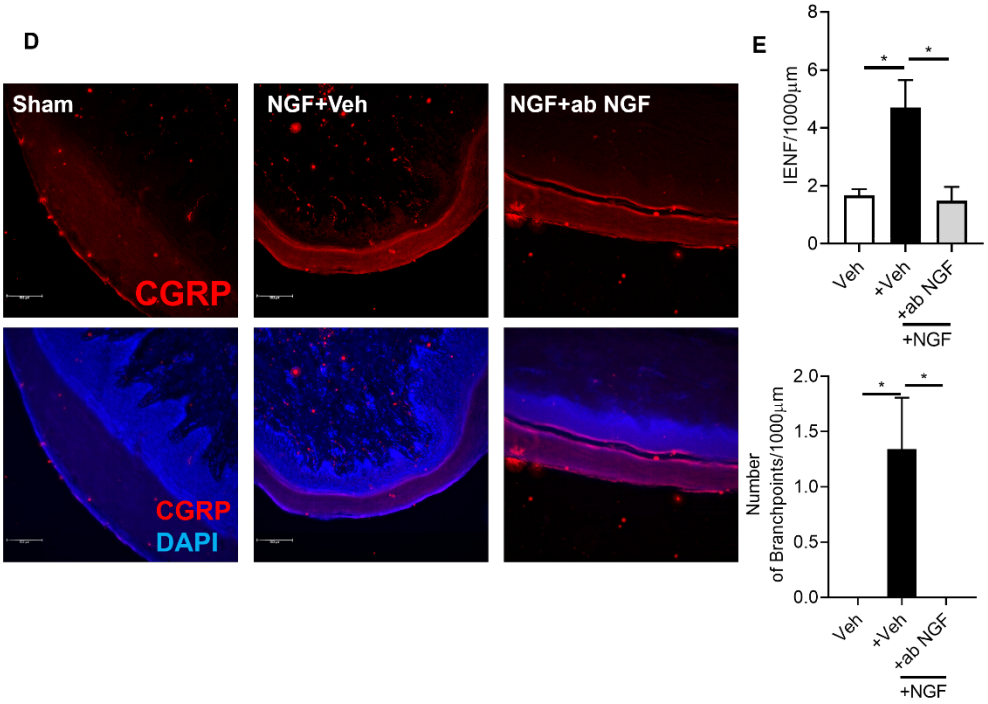
D
Sham
NGF+Veh
NGF+ab NGF
CGRP
CGRP
DAPI
E
IENF/1000μm
Veh
+Veh
+ab NGF
+NGF
Number
of Branchpoints/1000μm
Veh
+Veh
+ab NGF
+NGF

Figure 5

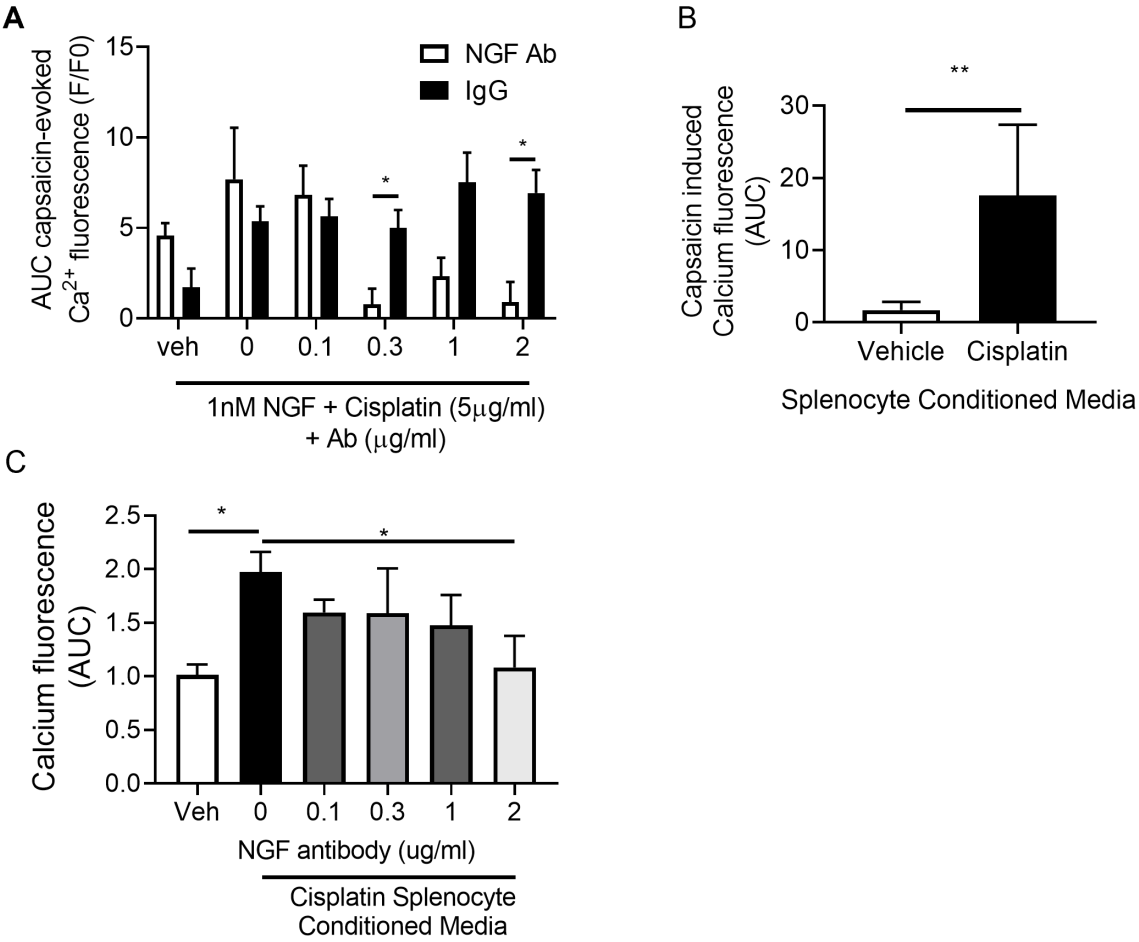
A
AUC capsaicin-evoked
Ca2+ fluorescence (F/F0)
15
10
5
0
NGF Ab
IgG
*
*
veh
0
0.1
0.3
1
2
1nM NGF + Cisplatin (5μg/ml)
+ Ab (μg/ml)
B
Capsaicin induced
Calcium fluorescence
(AUC)
30
20
10
0
**
Vehicle
Cisplatin
Splenocyte Conditioned Media
C
Calcium fluorescence
(AUC)
2.5
2.0
1.5
1.0
0.5
0.0
*
*
Veh
0
0.1
0.3
1
2
NGF antibody (ug/ml)
Cisplatin Splenocyte
Conditioned Media

Figure 6

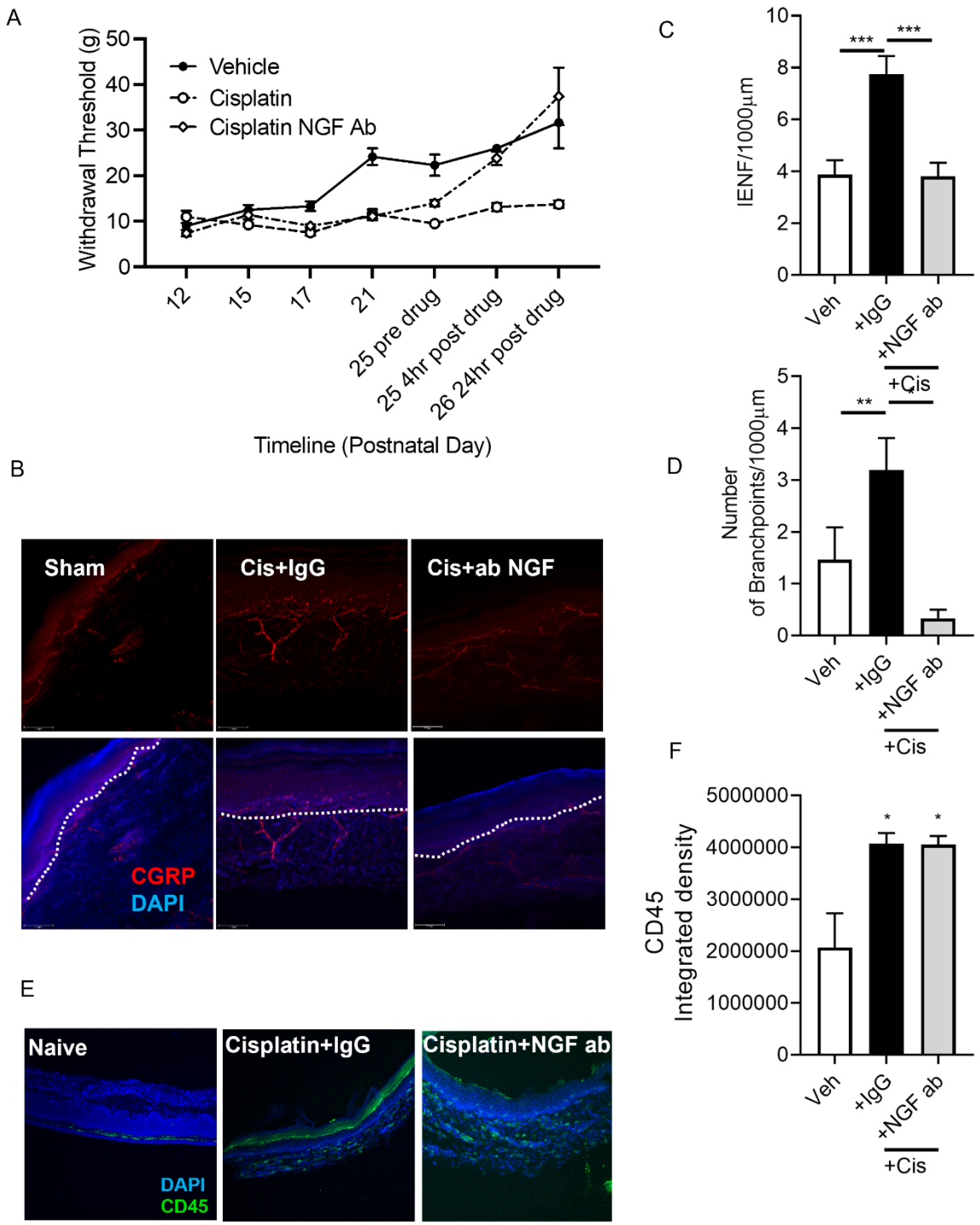
A
Withdrawal Threshold (g)
50
40
30
20
10
0
Vehicle
Cisplatin
Cisplatin NGF Ab
12
15
17
21
25 pre drug
25 4hr post drug
26 24hr post drug
Timeline (Postnatal Day)
B
Sham
Cis+IgG
Cis+ab NGF
CGRP
DAPI
E
Naive
Cisplatin+IgG
Cisplatin+NGF ab
DAPI
CD45
C
IENF/1000µm
10
8
6
4
2
0
***
***
Veh
+IgG
+NGF ab
+Cis
D
Number
of Branchpoints/1000µm
5
4
3
2
1
0
**
Veh
+IgG
+NGF ab
+Cis
F
CD45
Integrated density
5000000
4000000
3000000
2000000
1000000
0
*
*
Veh
+IgG
+NGF ab
+Cis